SERI/TP-217-3243
UC Category: 60
DE88001110

Preliminary Results from the Dynamic Response Testing of the Howden 330-kW HAWT

S.M. Hock
T.E. Hausfeld
G. Hampson
R.W. Thresher

October 1987

Prepared for Windpower '87
San Francisco, California
5-8 October, 1987

Prepared under Task No. 4845.20

Solar Energy Research Institute
A Division of Midwest Research Institute

1617 Cole Boulevard
Golden, Colorado 80401-3393

Prepared for the
U.S. Department of Energy
Contract No. DE-AC02-83CH10093

NOTICE

Printed in the United States of America
Available from:
National Technical Information Service
U.S. Department of Commerce
5285 Port Royal Road
Springfield, VA 22161

Price: Microfiche A01
Printed Copy A02

Codes are used for pricing all publications. The code is determined by the number of pages in the publication. Information pertaining to the pricing codes can be found in the current issue of the following publications, which are generally available in most libraries: *Energy Research Abstracts. (ERA); Government Reports Announcements* and Index (*GRA* and I); *Scientific and Technical Abstract Reports (STAR):* and publication. NTIS-PR-360 available from NTIS at the above address.

PRELIMINARY RESULTS FROM THE DYNAMIC RESPONSE TESTING OF THE HOWDEN 330-kW HAWT

S. M. Hock
T. E. Hausfeld
G. Hampson
R. W. Thresher
Solar Energy Research Institute
Wind Research Branch
1617 Cole Blvd., Golden, Colo., 80401

ABSTRACT

As part of the Department of Energy (DOE) Cooperative Field Test Program, Southern California Edison (SCE) and the Solar Energy Research Institute (SERI) performed a comprehensive dynamic response test on the 330-kW, horizontal-axis wind turbine (HAWT) manufactured by the James Howden Company. This paper presents a preliminary analysis of some data from the test. The data were analyzed using different statistical approaches. First, the mean turbine operating conditions were analyzed using the method of bins. In addition, azimuth averaging was used to separate the deterministic responses from the stochastic responses. The results presented include comparisons of mean power and load versus wind speed. Deterministic rotor-bending loads are plotted as a function of blade azimuth position. Auto-spectral density plots are also computed for the stochastic portion of the rotor blade root-bending moments to determine their dynamic responses to turbulent wind inputs.

INTRODUCTION

Under the DOE Cooperative Field Test Program, SERI and SCE conducted a measurement program that included a complement of structural load measurements to characterize the dynamic response of the turbine, as well as an array of wind sensors to characterize both the mean and turbulent wind field in front of the turbine.

TURBINE DESCRIPTION

The field test turbine, manufactured by James Howden and Company, was a three-bladed, upwind machine with a rigid hub and wood/epoxy blades. It was rated at 330 kW in a hub-height wind speed of 32.4 mph (14.5 m/s) and was designed to operate in cut-in and cut-out wind speeds of 13.4 and 62.6 mph (6.0 and 28.0 m/s), respectively. The rotor diameter was 85.3 ft (26 m) and the rotor speed was 42 rpm. The blades were tapered and twisted, with a maximum chord of 4.82 ft (1.47 m) and a maximum twist angle of 16°; the blade tapered to a 2.6-ft (0.8-m) chord and 0° twist at the blade tip. The blade airfoil section was a GA(W)-1, 17% thick. The blade dimensions are shown in Table 1.

The rotor axis centerline above the ground was at 79.1 ft (24.1 m), and the rotor coning angle (precone) was 0°. The tower diameter was 5.9 ft (1.8 m), and the distance from the yaw axis to the rotor plane was 11.5 ft (3.5 m). Figure 1 is a sketch of the turbine, taken from [1].

TABLE 1. HOWDEN WIND TURBINE BLADE DIMENSIONS (FROM [1])

Radius (ft)	Chord (ft)	Twist* (deg.)	Notes
1.31	2.10	16.0	Root (fixed pitch)
9.84	4.80	16.0	Blade "knee"
36.10	3.10	3.2	Tip joint
42.60	2.60	0.0	Tip (pitchable)

*Toward feather.

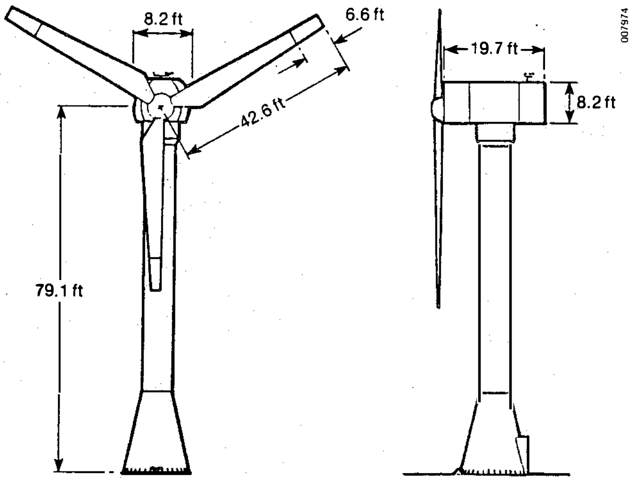

Figure 1. THE HOWDEN HWP 330/26 WIND TURBINE

THE INSTRUMENTATION

A total of 44 channels of data were recorded in multiplexed form on a Honeywell 101 14-channel tape recorder. The 13 channels of machine data listed in Table 2 were collected through the Howden data system. The effective cut-off frequency of the Howden data system was about 30 Hz. The 31 channels of atmospheric data were low-pass filtered at 10 Hz. The wind data of interest for this study came from the vertical-plane array using three-axis UVW Gill propeller anemometers located 68.9 ft (21 m) [or 0.8 rotor diameters (D)] due west and upwind of the turbine in the prevailing wind direction. The numbering scheme for the anemometers on this array is shown in Figure 2. In addition, there was a single UVW Gill propeller anemometer at hub height, located 2D upwind. The primary machine data used for this study were the power, tip pitch position, blade azimuth, and blade-bending moments at the 4.92-ft (1.5-m) and 27.1-ft (8.25-m) spanwise stations. The analog data collected during the test were digitized at SERI using the NEFF 720 system at a sample rate of 41.67 Hz. This high rate was necessary to accurately resolve the blade angular position for azimuth averaging.

TABLE 2. TURBINE MEASUREMENTS

Channel*	Description
1	Blade azimuth position
2	Blade flap moment at 1.5 m
3	Blade flap moment at 4.5 m
4	Blade flap moment at 8.27 m
5	Blade flap moment at 9.75 m
6	Blade edge moment at 1.5 m
8	Rotor shaft torque
9	Tip position
10	Yaw angle
12	Generator power
41	Blade edge moment at 4.5 m
42	Tower fore-aft moment (7.95 m above base)
43	Tower top displacement

*The remaining 31 channels were wind inflow measurements.

STUDY DATA CASES

The data selected for this study consist of five 10-min data cases covering a wide range of machine operating conditions. These data cases cover a wind-speed range from cut-in to well above rated power, while the turbine is regulating power output using the tip controls. In addition, the data case for run 1, segment 5 (expressed as Case 1-5), has a yaw angle of 14°. The operating statistics for these five cases are summarized in Table 3.

The five data cases were examined using three different statistical approaches. First, the mean turbine responses were computed using the method of

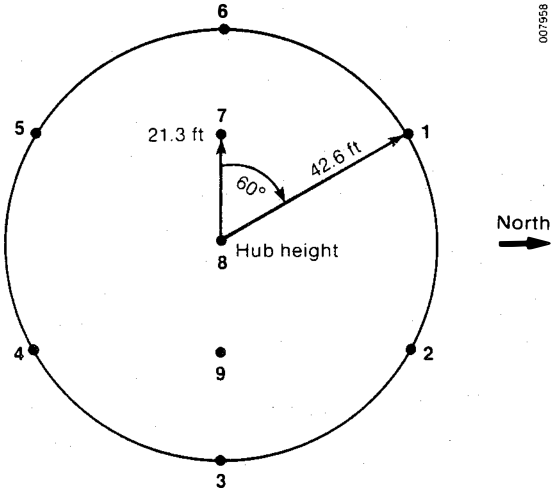

Figure 2. **PLACEMENT AND NUMBERING OF THE UVW GILL ANEMOMETERS ON THE ARRAY (LOOKING UPWIND TO THE WEST)**

TABLE 3. OPERATING CONDITIONS FOR THE FIVE 10-MINUTE DATA CASES

Data case (run-segment)	Wind speed (m/s)		Turb. int.	Power (kW)		Tip pitch (deg.)	
	$\bar{V}_8$	$\bar{V}_{disk}^*$	$(\sigma/\bar{V}_8)^{**}$	Mean	σ	Mean	σ
3-5	9.65	9.86	0.13	119	35	0.3	0.1
13-1	12.63	13.06	0.13	241	60	0.5	1.8
12-7	10.45	10.79	0.18	169	64	0.0	0.1
1-5	13.38	13.65	0.12	240	52	0.7	1.6
17-4	16.63	16.88	0.13	298	25	10.9	4.5

*$\bar{V}_{disk} = (\bar{V}_1 + \bar{V}_2 + \bar{V}_4 + \bar{V}_5)/4$, where $\bar{V}_i$ = 10-min wind-speed average.
**σ = standard deviation of wind speed.

bins. Next, the deterministic and stochastic portions of the time-series turbine responses were separated using azimuth averaging. Then, the deterministic turbine response could be determined. Finally, spectral analysis was used to look briefly at the random blade responses.

MEAN TURBINE RESPONSES

The turbine power output, pitch angle motion, and mean root flap moments at the 1.5-m and 8.25-m blade stations were determined using the method of bins. The data were preaveraged over a time period equal to one rotor revolution to eliminate higher harmonic responses. In addition, the wind-speed signal to be used for binning the turbine responses was formed by computing a rotor disk averaged wind signal,

$$\hat{V}_{disk} = (\hat{V}_1 + \hat{V}_2 + \hat{V}_4 + \hat{V}_5)/4 ,$$

where each of the V_i signals was preaveraged over a period of one rotor revolution. The original plan was to compute other disk-averaged wind signals and try several preaveraging times. However, the results looked satisfactory; experimenting with other preaveraging times was unnecessary. The turbine responses were binned into 0.5-m/s wind bins, and bins containing less than 10 data points were discarded. Also, no density correction or pressure adjustments were made to the data.

Figures 3 through 6 present the mean turbine responses using this method-of-bins computation. Figure 3's curve is power versus wind speed and compares the results with Howden's predictions as given in [1]. Figure 4 shows the tip pitch angle versus wind speed and reveals some interesting behavior for the data case where the wind speed is well above rated. Since the blade tip is operated as a drag device in deep stall (where our fundamental understanding is limited), it is not unexpected to observe behavior that deviates from the predictions. Figures 5 and 6 present the mean flap-bending moments as a function of wind speed for the blade root at the 1.5-m and 8.25-m blade stations. The mean experimental loads seem somewhat higher than the Howden predictions. Careful examination of the data for Case 1-5 (the line with the diamond-shaped symbols) shows that it falls slightly below the other results for power and mean bending moments. Case 1-5 has a 14° yaw error.

DETERMINISTIC TURBINE RESPONSES

It is assumed that for stationary operating conditions of the test turbine the deterministic and stochastic loads can be separated by the process of azimuth averaging. Azimuth averaging is accomplished by binning the measured forces with respect to the azimuth angle of the rotor blade for a large number of rotor cycles. The results of this averaging process are signals that are periodic with rotor angle and provide an estimate of the deterministic forces acting over the averaging time. The stochastic forces are then given by subtracting the azimuth-averaged signals from the original signals.

Azimuth-averaged rotor-blade bending moments were determined by binning the time-series data on blade azimuth angle for each 10-min data case (420 revolutions). Figure 7 shows a plot of the azimuth-averaged (1.5-m) root-bending moment for Case 3-5. The figure includes the bin means, plus and minus one bin standard deviation, the bin maximum and minimum, and a sixth-order Fourier series fit to the azimuth average. Notice that the standard deviation is approximately constant with azimuth angle, hopefully indicating a stationary process for the random part of the bending-moment signal. Figure 8 shows the azimuth-averaged root-bending moment (at the 1.5-m station) for all five data cases. Observe that the waveforms are very similar and change shape only slightly with increasing mean level (wind speed), except for Case 1-5. The azimuth averaging clearly shows the stronger one-per-revolution (1P) bending-moment content for this 14° yaw case. Figure 9 shows the azimuth-averaged bending moment for the blade station at 8.25 m for Case 3-5. Figure 10 plots the bending moment at the 8.25-m blade station for all of the data cases. Notice that the waveform for the high yaw error of Case 1-5 is again clearly evident.

The harmonic contents of the azimuth-averaged root-bending-moment waveforms shown in Figure 8 are illustrated in the bar chart of Figure 11. The harmonic contents for the bending moment at the 8.25-m blade station are given in Figure 12. Both figures show the same general trends. There are significant 1P and 2P bending moments that are approximately the same percentage of the mean moment for all wind speeds. The single exception is the high-yaw-error case (1-5), which has a higher 1P moment. However, the 2P moment is consistent with the other cases.

THE STOCHASTIC TURBINE RESPONSES

The stochastic rotor loads were obtained by subtracting the azimuth-averaged signal from the original time series. These time series were then analyzed spectrally. Figure 13 is an auto-spectral density plot for the stochastic portion of the root-bending moment for Case 12-7, which has the highest turbulence. Figure 14 is an auto-spectral density plot for the stochastic portion of the root-bending moment for a high-wind-speed case. To understand the various peaks in these plots, it is useful to know the placement of natural frequencies for the turbine. Howden's predicted frequencies are given in Table 4. The spectral plots clearly identify the 1P and 2P blade-passage frequencies. The natural frequencies around 1.4 Hz are probably buried in the rather broad 2P spike shown in the spectral plots. The small, narrow spike at 1.8 Hz is probably the rotor flap/tower mode identified as Mode 5 in Table 4. The small spike at about 3.2 Hz may be the blade flap mode identified in Table 4 as Mode 6. Notice that even though the turbine is three-bladed, the 3P spike is very small.

To estimate the significance of the stochastic root-bending moment loads, the area under the auto-spectral density plots was calculated in three frequency bands. The area is the contribution to the signal variance in that frequency band. Table 5 presents the standard deviation (square root of the variance) for the low-frequency, 1P, and 2P bands for the auto-spectral density plots in Figures 13 and 14. All three bands appear to be making significant contributions to the cyclic bending moments; also, taken as a sum, the stochastic portion of the signal is about 75% of the variance of the bending moment for these two cases.

CONCLUSIONS

Data from the dynamic response testing of the SCE-owned Howden 330-kW HAWT have been examined using

TABLE 4. PREDICTED NATURAL FREQUENCIES (NONROTATING)

Mode	Frequency Hz	Frequency Per rev.	Mode Shape
1	1.33	1.90	Rotor flap - tower (fore to aft)
2	1.43	2.04	Rotor flap (no tower)
3	1.43	2.04	Rotor flap (no tower)
4	1.53	2.20	Tower - rotor side-to-side
5	1.72	2.50	Rotor flap - tower (fore to aft)
6	3.43	4.90	Blade flap

TABLE 5. VARIANCE FOR THE STOCHASTIC ROOT-BENDING MOMENTS FOR THREE FREQUENCY BANDS

Data case (run-segment)	Description	Low-frequency* (0-0.39 Hz)		1P band (0.39-1.0 Hz)		2P band (1.0-1.6 Hz)	
		$\sigma^2(\text{ft-lb})^2$	$(\frac{\sigma}{\sigma_T})^2$	$\sigma^2(\text{ft-lb})^2$	$(\frac{\sigma}{\sigma_T})^2$	$\sigma^2(\text{ft-lb})^2$	$(\frac{\sigma}{\sigma_T})^2$
12-7	High turbulence	$(12430)^2$	50%	$(4530)^2$	13%	$(5521)^2$	19%
17-4	High wind	$(8034)^2$	16%	$(6543)^2$	19%	$(7978)^2$	29%

*σ_T = standard deviation of the raw time-series bending moment containing both deterministic and stochastic loads.

three different analyses. The mean loads and performance were estimated using the method of bins. Azimuth averaging was used to separate the deterministic and stochastic portions of the turbine responses, and spectral analysis was applied to develop insight into the stochastic responses. The binning analysis defined the mean turbine operating states. Preaveraging over one revolution and averaging four anemometers spanning the rotor disk gave good results for the mean response curves.

Azimuth averaging separated the deterministic and random signals. The deterministic signals obtained this way showed a smooth transition of waveform with increasing wind speed, and the high-yaw-error data showed a distinctly different waveform with a much larger 1P harmonic content. The stochastic portion of the root-bending moment time series was analyzed using spectral analysis and allowed the key rotor responses to be identified. In addition, the stochastic contributions to the cyclic loads were analyzed and found to be significant not only at frequencies above 1P, but at lower frequencies as well.

Readers interested in additional analysis or a comparison of these test results with analytical predictions using the Force and Loads Analysis Program (FLAP) rotor code are referred to [2].

REFERENCES

1. Redmond, I., Anderson, C.G., and Jamieson, P., "Dynamic Response of a 330kW Horizontal Axis Wind Turbine Generator," unpublished report by James Howden and Co. LTD, under SERI cooperative agreement No. DE-FC02-85CH10249.

2. Wright, A.D., and Thresher, R.W., "Accurate Rotor Loads Prediction Using the FLAP Dynamics Code," presented at Windpower '87, San Francisco, CA, October 5-8, 1987.

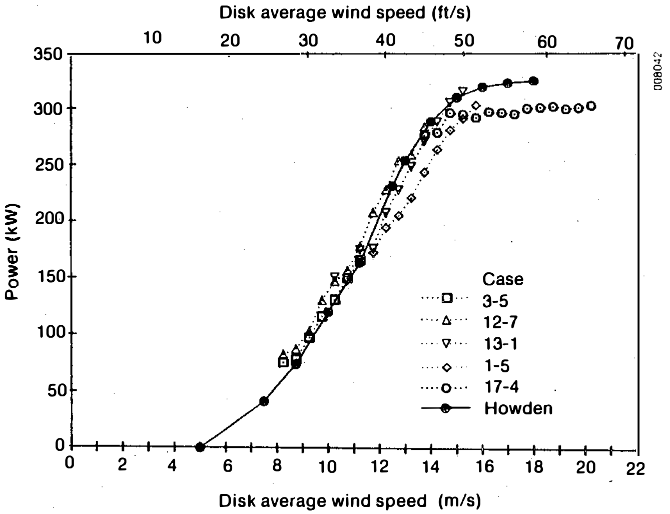

Figure 3. MEAN POWER CURVE COMPUTED USING THE METHOD OF BINS WITH A PREAVERAGING TIME OF ONE ROTOR REVOLUTION

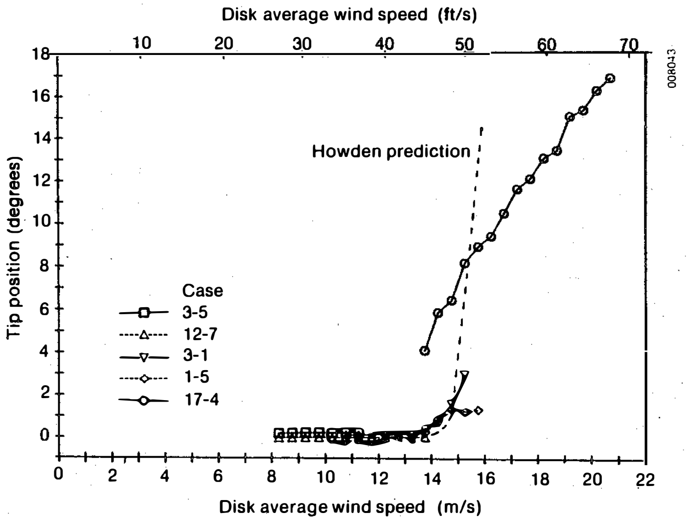

Figure 4. MEAN TIP PITCH POSITION AS A FUNCTION OF WIND SPEED

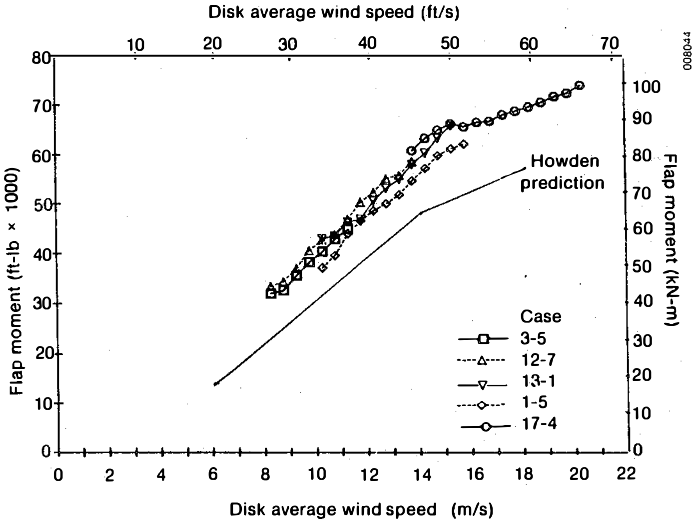

Figure 5. MEAN FLAP-BENDING MOMENTS AT THE 1.5-m BLADE STATION

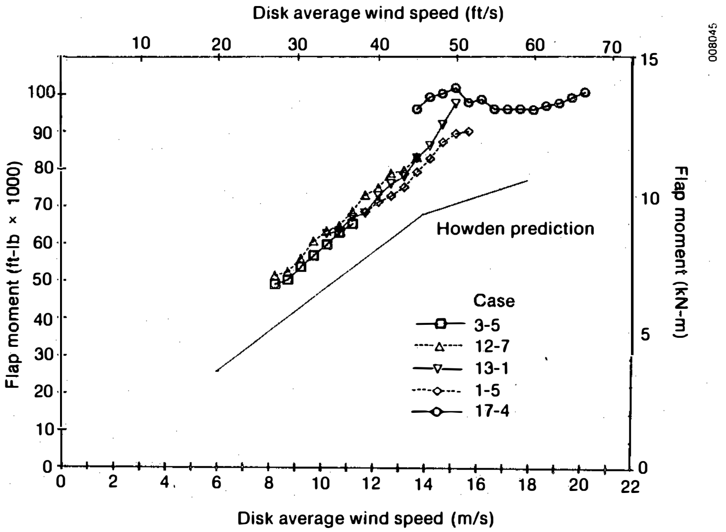

Figure 6. MEAN FLAP-BENDING MOMENTS AT THE 8.25-m BLADE STATION

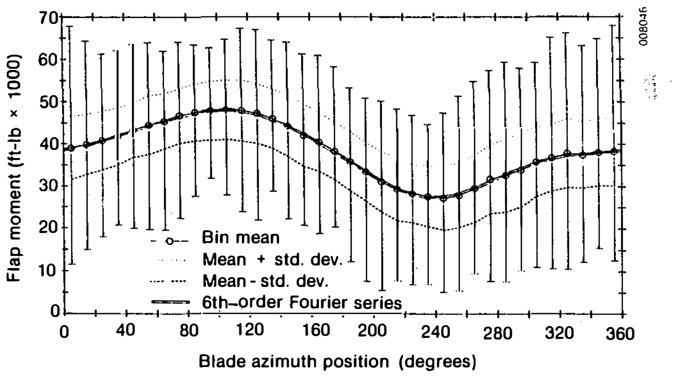

Figure 7. AZIMUTH-AVERAGED ROOT-BENDING MOMENT (1.5-m BLADE STATION) FOR CASE 3-5

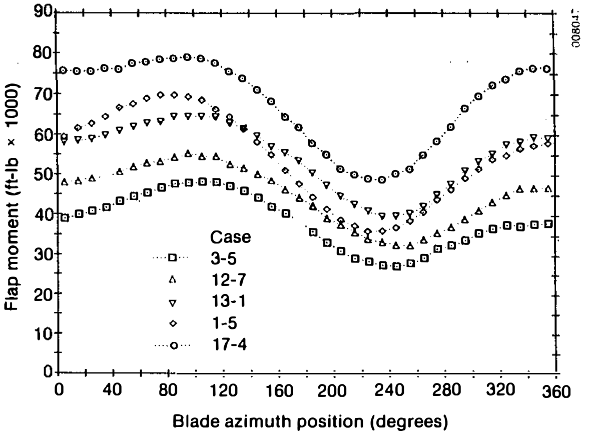

Figure 8. COMPARISON OF AZIMUTH-AVERAGED ROOT MOMENTS

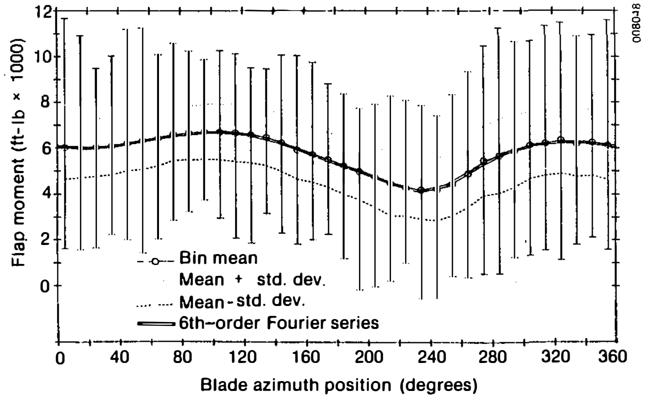

Figure 9. AZIMUTH-AVERAGED ROOT-BENDING MOMENT (8.25-m BLADE STATION) FOR CASE 3-5

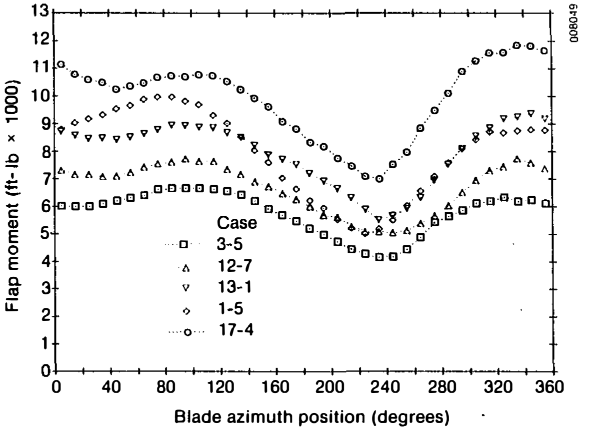

Figure 10. COMPARISON OF BENDING MOMENTS (8.25-m BLADE STATION)